

Unveiling E_6 SSM Scalar Diquarks at the HL-LHC

M. Ali^{a,b,c}, S. Khalil^d, S. Moretti^{e,f}, S. Munir^{g,h}, H. Waltari^e

^a East African Institute for Fundamental Research (ICTP-EAIFR), University of Rwanda, Kigali, Rwanda

^b The Abdus Salam ICTP, Strada Costiera 11, 34135, Trieste, Italy

^c SISSA International School for Advanced Studies, Via Bonomea 265, 34136, Trieste, Italy

^d Center for Fundamental Physics, Zewail City of Science and Technology, 6 October City, Giza, Egypt

^e Department of Physics and Astronomy, Uppsala University, Box 516, SE-751 20 Uppsala, Sweden

^f School of Physics & Astronomy, University of Southampton, Southampton SO17 1BJ, UK

^g Department of Physics, Faculty of Natural Sciences and Mathematics, St. Olaf College, Northfield, Minnesota 55057, USA

^h Physics Department, Augustana University, Sioux Falls, South Dakota 57197, USA

mali@eaifr.org, skhalil@zewailcity.edu.eg, stefano.moretti@cern.ch, shoaib.munir@augie.edu,
harri.waltari@physics.uu.se

Abstract

We investigate the phenomenology of scalar diquarks with sub-TeV masses within the framework of the E_6 Supersymmetric Standard Model (E_6 SSM) at the Large Hadron Collider (LHC). Focusing on the lightest of the six diquarks predicted by the model, we select some representative low masses for them in a parameter space region consistent with experimental constraints from direct searches for additional Higgs boson(s), Cold Dark Matter (CDM), and supersymmetry, as well as from flavor physics analyses. Using Monte Carlo (MC) simulations, we assess these benchmark points against the latest LHC results corresponding to an integrated luminosity of 140 fb^{-1} . We further evaluate the signal significance of the pair-production of these diquarks, when each of them decays into tb pairs, at the $\sqrt{s} = 13 \text{ TeV}$ LHC Run 3 with design integrated luminosity of 300 fb^{-1} , and also at the 3000 fb^{-1} High-Luminosity LHC (HL-LHC). Our analysis yields a statistical significance exceeding 3σ at the HL-LHC for diquark masses up to 1 TeV , indicating promising prospects for their discovery.

1 Introduction

The Standard Model (SM) has proven to be highly effective in elucidating most of the observations made by particle as well as astro-particle physics experiments thus far. Nevertheless, due to factors such as the hierarchy problem, the nature of CDM, CP violation (CPV), and the matter-antimatter asymmetry of the Universe, it is widely acknowledged that the SM represents only the low-energy limit of an extended theoretical framework. Since its launch, the LHC has been vastly anticipated to directly unveil new-physics (NP) particles. That has not occurred yet, possibly because the scale at which NP exists lies beyond the current reach of the LHC, and/or perhaps because NP is different from its most sought after types, that are predicted by some well-established and appealing frameworks.

One potential way in which NP can manifest itself is a diquark – a particle that only interacts with (and hence decays into) a pair of quarks. Such a particle appears in E_6 [1] as well as Pati-Salam ($SU(4)_C \times SU(2)_L \times SU(2)_R$) [2] Grand Unified Theories (GUTs), and in R -parity violating SUSY models [3]. It can contribute to $n-\bar{n}$ oscillations [4–9], and to various other similar processes [10–12]. Diquarks have also been employed to address the strong CP problem, and they can potentially impact both indirect (ϵ_K) and direct (ϵ'/ϵ) CPV in kaons [13, 14]. Furthermore, diquark provided one of the plausible explanations of the forward-backward asymmetry observed in $t\bar{t}$ production at the Tevatron [15–20].

Under $SU(3)_C$, quarks are $\mathbf{3}$ s, so that

$$\begin{aligned} \mathbf{3} \otimes \mathbf{3} &= \mathbf{6} \oplus \bar{\mathbf{3}}, \\ \mathbf{3} \otimes \bar{\mathbf{3}} &= \mathbf{8} \oplus \mathbf{1}, \end{aligned} \tag{1}$$

implying that the color scalar exotic states may transform as sextets, anti-triplets, octets or singlets. The Lorentz-invariant interactions of these colored scalar exotic states with a Dirac spinor, $\psi = P_L\psi + P_R\psi$, with $P_{L,R}$ denoting the helicity projection operators, are given as

$$\bar{\psi}\psi\phi + \bar{\psi}^c\psi\Phi. \tag{2}$$

The first term preserves $B + L^1$ with ϕ being an octet or a singlet that only couples to spinors with different chiralities. The second term above clearly violates $B + L$ and Φ , which transforms as a sextet or an anti-triplet, and only couples to two quarks with the same chirality, is identified as a diquark. Here Φ carries a net baryon number, $B = \pm\frac{2}{3}$, and it is a scalar if it transforms under $SU(2)_L$ either as a singlet or a triplet, but a vector if it transforms as a doublet.

The Yukawa Lagrangian of a scalar $\Phi \equiv S$ is written as

$$\mathcal{L}_S = \lambda_{ij}^{(\alpha)} \bar{\psi}_i^c P_{L,R} \psi_j S_\alpha + h.c., \tag{3}$$

while for the vector $\Phi \equiv V^\mu$ it is

$$\mathcal{L}_V = \eta_{ij}^{(\beta)} \bar{\psi}_i^c \gamma_\mu P_{L,R} \psi_j V_\beta^\mu + h.c. \tag{4}$$

Here λ and η denote the couplings of S and A^μ , respectively, and the i and j indices reflect the quark flavors. In Tab. 1, we show the classification of the ($\alpha = 1 - 8$) scalar and ($\beta = 1 - 4$) vector diquarks according to their charges under the SM gauge group. The sextets are symmetric in color, while the triplets are antisymmetric. The interchange of quarks plays a crucial role in determining the couplings of the diquark. If the diquark state is antisymmetric under the exchange of two quarks, it only couples to two quarks with different flavors, but not to same-flavor quark pairs.

Diquark type	$SU(3)_C \times SU(2)_L \times U(1)_Y$ charges	Couplings
S_1	$(6, 3, +1/3)$	$Q_L Q_L$
S_2	$(\bar{3}, 3, +1/3)$	$Q_L Q_L$
S_3	$(6, 1, +1/3)$	$Q_L Q_L, u_R u_R$
S_4	$(\bar{3}, 1, +1/3)$	$Q_L Q_L, u_R u_R$
S_5	$(6, 1, +4/3)$	$u_R u_R$
S_6	$(\bar{3}, 1, +4/3)$	$u_R u_R$
S_7	$(6, 1, -2/3)$	$d_R d_R$
S_8	$(\bar{3}, 1, -2/3)$	$d_R d_R$
V_1^μ	$(\bar{6}, 2, +1/3)$	$Q_L \gamma_\mu d_R$
V_2^μ	$(3, 2, +1/3)$	$Q_L \gamma_\mu d_R$
V_3^μ	$(\bar{6}, 2, -5/3)$	$Q_L \gamma_\mu u_R$
V_4^μ	$(3, 2, -5/3)$	$Q_L \gamma_\mu u_R$

Table 1: Charges of all possible scalar and vector diquarks under the SM gauge group, and the quark chiral pairs they couple to.

Thus, the antisymmetry of the diquark state under the SM gauge group implies an antisymmetry under flavor as well [21].

The prospects of the direct observation of a scalar diquark at the LHC have been previously investigated in [2, 4, 22–27], but such a particle remains elusive to this day. These studies have, however, explored the production of a single diquark, while its pair-production remains largely unexplored. In this study we conduct a phenomenological analysis of the production of a pair of diquarks of the type S_4 , naturally predicted by the E_6 SSM [28], which is one of the most well-founded E_6 -inspired SUSY models. It offers a highly appealing theoretical resolution to the μ problem encountered in the Minimal supersymmetric Standard Model (MSSM), thanks to the $U(1)_N$ gauge symmetry that prohibits the presence of bilinear terms for the Higgs supermultiplets in the superpotential. We test the consistency of the lightest diquark, referred to as D here, predicted by the E_6 SSM with the exclusion bounds from the LHC on an S_4 produced singly in association with a heavy charged Higgs boson, and decaying into a tb pair. We then reconstruct a $D\bar{D}$ pair by applying a set of well-defined selection cuts on the semi-leptonic decays of $t\bar{t}$, in an attempt to establish the discovery prospects of D states at the LHC. Our signal-to-background analysis predicts a sizeable statistical significance of their signature in the $t\bar{t}b\bar{b}$ channel at the HL-LHC.

The paper is structured as follows. Section 2 describes the E_6 SSM, detailing in particular the characteristics of the scalar diquarks in it. In Section 3 we discuss our Monte Carlo (MC) analysis, performed to first evaluate the constraints on the D mass from the most recent LHC searches of the S_4 . Section 4 then outlines our event selection and methodology for reconstructing the $D\bar{D}$ pair. Finally, in Section 5 we present our conclusions.

¹Hereafter, $B(L)$ denotes the Baryon(Lepton) number, so that $B + L$ is effectively the global fermion number.

2 The E_6 SSM

The E_6 group can be broken down to the SM along with one extra surviving $U(1)'$ symmetry as

$$\begin{aligned} E_6 &\xrightarrow{M_{\text{GUT}}} SO(10) \times U(1)_\psi \\ &\xrightarrow{M_*} SU(5) \times U(1)_\chi \times U(1)_\psi \\ &\xrightarrow{M_{**}} SU(3)_C \times SU(2)_L \times U(1)_Y \times U(1)', \end{aligned}$$

where $U(1)' = U(1)_\chi \cos \theta + U(1)_\psi \sin \theta$. The E_6 SSM is obtained for $\tan \theta = \sqrt{15}$, and thus implies $U(1)' \equiv U(1)_N$, under which the right-handed neutrinos transform trivially. In this SUSY model, the cancellation of anomalies occurs automatically if the particle spectrum at low energy includes three complete 27-dimensional representations of E_6 , which is decomposed under $SU(5) \times U(1)_N$ as

$$27_i \rightarrow \left(10, \frac{1}{\sqrt{40}}\right)_i + \left(\bar{5}, \frac{2}{\sqrt{40}}\right)_i + \left(\bar{5}, \frac{-3}{\sqrt{40}}\right)_i + \left(5, \frac{-2}{\sqrt{40}}\right)_i + \left(1, \frac{5}{\sqrt{40}}\right)_i + (1, 0)_i, \quad (5)$$

with $i = 1, 2, 3$. Each 27-plet (which is in fact a supermultiplet) consists of one generation of SM fermions (the first two terms on the right), up- and down-type Higgs doublets and color triplet scalars D and \bar{D} (terms 3 and 4), a SM-singlet field with a non-zero $U(1)_N$ charge (term 5), and a right-handed neutrino (term 6) - along with their respective spin-1/2 superpartners.

Excluding non-renormalizable interactions, the most general gauge invariant low energy superpotential of the E_6 SSM can be formulated as

$$W_{E_6\text{SSM}} = W_0 + W_1 + W_2, \quad (6)$$

where

$$\begin{aligned} W_0 &= \lambda_i \Phi (H_i^d H_i^u) + \kappa_i \Phi_i (D_i \bar{D}_i) \\ &\quad + \frac{1}{2} M_i N_i^c N_i^c + h_{ij} N_i^c (H_u L_j) + W_{\text{MSSM}}(\mu = 0), \\ W_1 &= g_{ijk}^Q D_i Q_{L_j} Q_{L_k} + g_{ijk}^q \bar{D}_i d_{R_j}^c u_{R_k}^c, \\ W_2 &= g_{ijk}^N N_i^c D_j d_{R_k}^c + g_{ijk}^E e_{R_i}^c D_j u_{R_k}^c + g_{ijk}^Q Q_{L_i} L_{L_j} \bar{D}_k, \end{aligned} \quad (7)$$

with summation over repeated family indices ($i, j, k = 1, 2, 3$) implied. The supermultiplets in the above equation are the SM singlets Φ_i , Higgs doublets H_{d_i} and H_{u_i} , right-handed neutrinos N_i^c , charged leptons e_i^c , up-type quarks u_i^c , and down-type quarks d_i^c , and the left-handed quark and charged-lepton doublets, Q_i and L_i , respectively.

The E_6 SSM is constructed so as to adhere to certain discrete symmetries. The presence of $U(1)_N$ automatically results in the conservation of $Z_2^M = (-1)^{3(B-L)}$, also known as R -parity, which ensures the stability of the Lightest Supersymmetric Particle (LSP) as a CDM candidate. Furthermore, in order to differentiate between the active and inert generations of the SM-singlets and the Higgs doublets, while also minimizing non-diagonal flavor transitions due to the Higgs sector, the superpotential is assumed to have an Z_2^H flavor symmetry [28, 29]. Since it forbids operators that allow the lightest exotic (s)quark to decay, it can only be an approximate symmetry, and Z_2^H -violating couplings less than 10^{-4} yield sufficient suppression of flavor-changing processes. Under this symmetry all the matter supermultiplets except $\Phi \equiv \Phi_3$, $H_d \equiv H_3^d$, and $H_u \equiv H_3^u$ are odd [28, 29]. Thus, H_α^d , H_α^u , and Φ_α , with $\alpha = 1, 2$, do not acquire vacuum expectation values (VEVs), and only H_u , H_d , and Φ constitute the Higgs sector. The VEV of Φ breaks the $U(1)_N$ symmetry, and generates the mass of the corresponding Z' boson as well as the effective μ -term.

Fields	Z_2^M	Z_2^H	Z_2^B	Z_2^L
$\Phi_\alpha, H_{d\alpha}, H_{u\alpha}$	+	-	+	+
Φ, H_d, H_u	+	+	+	+
$Q_{L_i}, d_{R_i}^c, u_{R_i}^c$	-	-	+	+
$L_{L_i}, e_{R_i}^c, N_i^c$	-	-	+	-
\overline{D}_i, D_i	+	-	+	+

Table 2: Field charges under the discrete symmetries of the E₆SSM.

Finally, W_1 and W_2 in Eq. (7) contain terms involving colored exotic states, which violate B and L in addition to Z_2^H , and can lead to rapid proton decay. One cannot define B and L of D_i and \overline{D}_i so that the complete Lagrangian is invariant under both the $U(1)_B$ and $U(1)_L$ global symmetries. However, for consistency of the proton lifetime in the model with the current experimental limits, either a Z_L^2 or Z_B^2 discrete symmetry can be imposed. Invariance under an exact Z_L^2 symmetry, under which all the superfields except the lepton ones are even, forbids the Yukawa interactions in W_2 . This reduces the E₆SSM superpotential to $W_0 + W_1$ only, and B -conservation implies that the S_4 -type scalars D_i and \overline{D}_i are diquarks. This is the E₆SSM variant under consideration here.² The behavior of the fields under the assumed symmetries is summarized in Tab. 2 for ease of understanding.

Choosing the field basis of the E₆SSM such that the Yukawa couplings of Φ to D_i and \overline{D}_i are flavor-diagonal results in mixing between their scalar components from the same family only. The calculation of the diquark masses therefore reduces to diagonalization of three 2×2 matrices

$$M^2(i) = \begin{pmatrix} M_{11}^2(i) & \mu_{D_i} X_{D_i} \\ \mu_{D_i} X_{D_i} & M_{22}^2(i) \end{pmatrix}, \quad (8)$$

$$\text{with } M_{11}^2(i) = m_{D_i}^2 + \mu_{D_i}^2 + \Delta_D, \quad M_{22}^2(i) = m_{\overline{D}_i}^2 + \mu_{D_i}^2 + \Delta_{\overline{D}}, \quad X_{D_i} = A_{\kappa_i} - \frac{\lambda_i}{\sqrt{2}\varphi} v_d v_u,$$

and $i = 1, 2, 3$. Here φ , v_d and v_u are the VEVs of Φ , H_d and H_u , respectively, $m_{D_i}^2$ are the soft scalar masses of D_i , and $m_{\overline{D}_i}^2$ those of \overline{D}_i . These mass parameters break global SUSY conditions, along with A_{κ_i} , the trilinear parameter associated with the coupling κ_i . The μ_{D_i} s above are the masses of the exotic fermionic counterparts of D_i , given (in the leading approximation) by

$$\mu_{D_i} = \frac{\kappa_i}{\sqrt{2}} \varphi, \quad (9)$$

while Δ_D and $\Delta_{\overline{D}}$ are the $U(1)_N$ D -term contributions to the diquark masses, set by $M_{Z'}^2$ as

$$\Delta_D \approx -\frac{1}{5} M_{Z'}^2, \quad \Delta_{\overline{D}} \approx -\frac{3}{10} M_{Z'}^2. \quad (10)$$

If we assume one of the two linear superpositions of the scalar components of D_3 and \overline{D}_3 supermultiplets (in analogy with the SUSY sector, and for index-alignment with the only active generation of the Higgs sector) to be the lightest S_4 -type diquark, which we denote by D for

²For $B = \pm \frac{1}{3}$ and $L = \pm 1$, W_1 is forbidden instead, and the E₆SSM superpotential is reduced to $W_0 + W_2$. In this variant of the model, the exotic scalars are S_1 -type leptoquarks, and their LHC phenomenology was studied recently in [30].

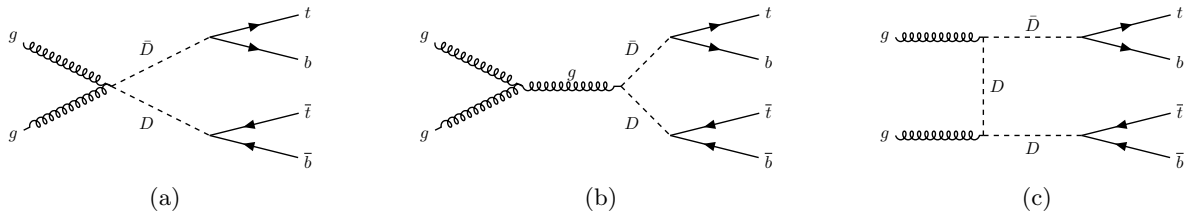


Figure 1: LO pair-production of S_4 -type diquarks ($D\bar{D}$) at the LHC.

simplification, its mass is given by

$$\begin{aligned}
 m_D^2 &= \frac{1}{2} \left[M_{11}^2(3) + \Delta_{11}(3) + M_{22}^2(3) + \Delta_{22}(3) \right. \\
 &\quad \left. - \sqrt{\left(M_{11}^2(3) + \Delta_{11}(3) - M_{22}^2(3) - \Delta_{22}(3) \right)^2 + 4 \left(\mu_{D_3} X_{D_3} + \Delta_{12}(3) \right)^2} \right], \quad (11)
 \end{aligned}$$

where Δ_{lm} ($l, m = 1, 2$) are the loop corrections to the four terms in the (symmetric) diquark mass matrix in Eq. (8) for the third generation.

3 Constraints from the LHC

Our analysis focuses on the pair production of a light $D\bar{D}$ pair.³ As noted in the previous section, the magnitude of mixing within each family of the diquark sector is governed by the parameters X_{D_i} and μ_{D_i} . While $\mu_{D_i} \propto \varphi$ is constrained by the collider limits on $M_{Z'} \approx g'_1 \tilde{Q}_\Phi \varphi$, with \tilde{Q}_Φ being the $U(1)_N$ charge of Φ , a large X_{D_i} can still lead to mixing effects substantial enough that D is one of the lightest SUSY particles, with a mass of the order of a few hundred GeV. Furthermore, if D has $O(10^{-3})$ couplings only to the third-generation fermions (and vanishing ones to the others), it can have $\text{BR}(D \rightarrow \bar{t}\bar{b}) = \text{BR}(\bar{D} \rightarrow t\bar{b}) \simeq 1$, where BR stands for Branching Ratio.

The most dominant processes contributing to the production of $D\bar{D}$ pairs at the LHC are shown in Fig. 1. For our analysis, we computed the leading order (LO) (inclusive) cross section for $D\bar{D}$ production using `MadGraph5_aMC@NLO` [31], as

$$gg \rightarrow D (\rightarrow \bar{t}\bar{b}) \bar{D} (\rightarrow t\bar{b}), \quad (12)$$

employing the `NNPDF31_lo_as_0118` parton distribution functions [32] for the gluons, followed by

$$\bar{t} \rightarrow \ell^- \nu \bar{b} \quad \text{and} \quad t \rightarrow jjb. \quad (13)$$

Evidently, this final state can also originate from the production of a charged Higgs boson in association with $\bar{t}\bar{b}$ pairs, and its total cross section is thus constrained by the corresponding searches in the ATLAS [33] and CMS [34] experiments. The ATLAS analysis pertains to a final state containing one charged lepton (e or μ) and jets, and the CMS analysis to an all-jet final state.

³Recall that we have identified D as the lightest of the six S_4 -type diquark mass eigenstates predicted by the E_6 SSM. Similarly, \bar{D} simply implies the lighter scalar diquark originating from the 27-plet containing the third-generation antifermions.

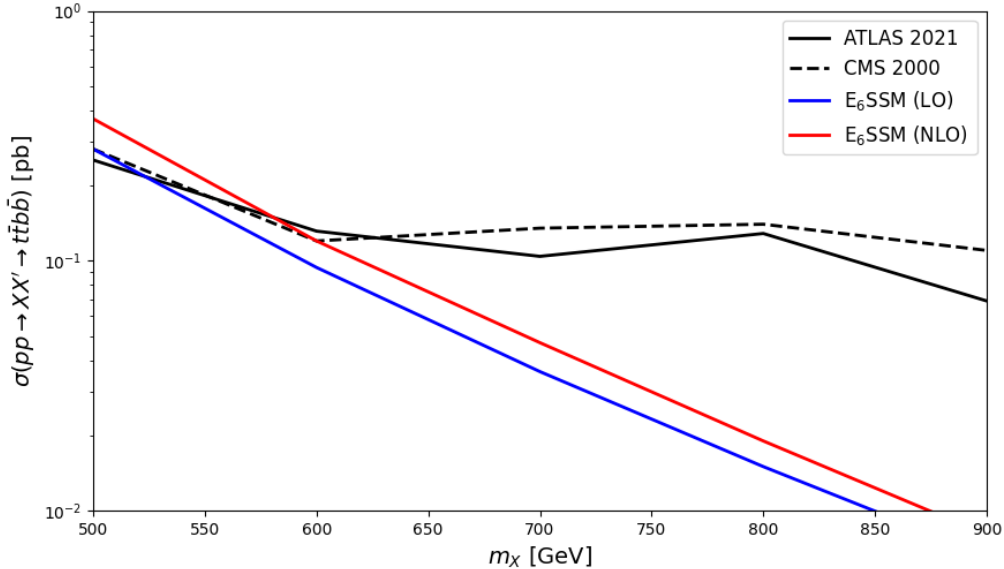


Figure 2: Exclusion contours in the $\{\sigma(t\bar{t}b\bar{b}), m_{H^\pm}\}$ plane from the ATLAS (solid black) and CMS (dashed black) data. The blue (red) line corresponds to the (N)LO cross section predicted for $t\bar{t}b\bar{b}$ production via $D\bar{D}$ in the E_6 SSM. The intersection of this line with a given contour is interpreted here as the m_D exclusion limit from the corresponding experiment.

At low energy, the phenomenological E_6 SSM contains a multitude of parameters. We fixed the minimal set of parameters, which includes

$$\tan\beta, g_N, \lambda, v_S, \lambda_3^T, M_i, M_{Q_i}, M_{U_i}, M_{D_i}^2, M_{\bar{D}_i}^2, M_{L_i}, M_{E_i}, T_f(i, j) [\equiv Y_f(i, j)A_f(i, j)],$$

$$M_{HuI}^2(\alpha, \beta), M_{HdI}^2(\alpha, \beta), E_{Mn}(i, j), E_\lambda(\alpha, \beta), E_\lambda^T(\alpha, \beta), g_{i,j,k}^Q, g_{i,j,k}^q, A_{\kappa_i}, \quad (14)$$

where $i, j, k = 1, 2, 3$, and $\alpha, \beta = 1, 2$, to non-zero values (only for the diagonal components in the case of matrices) in order to ensure self-consistency of the model. The values of the parameters related to the Higgs sector and the CDM were optimized for agreement of the corresponding observables with the experimental results. The masses of the physical diquarks can be controlled, for a given μ_{D_i} , by adjusting m_{D_i} and/or A_{κ_i} , as noted earlier. For simplicity, we fixed $m_{D_i}^2 = m_{\bar{D}_i}^2 = 2 \times 10^6 \text{ GeV}^2$ and varied A_{κ_i} slightly to obtain $m_D = 700 \text{ GeV}$, 800 GeV , and 900 GeV . The particle spectrum for this parameter space point was obtained by incorporating the E_6 MSSM into the public code SPheno-v4.0.4 [35,36] using the Mathematica package SARAH-v4.14.4 [37–40].

In Fig. 2 we show the exclusion contours in the $\{\sigma(t\bar{t}b\bar{b}), m_{H^\pm}\}$ plane obtained from the $H^\pm b\bar{t}$ searches at both CMS and ATLAS. Of the two searches, the CMS one gives a stronger exclusion limit of $\sim 600 \text{ GeV}$ on m_D corresponding to the above-noted configuration of the E_6 SSM parameters, for the $gg \rightarrow D\bar{D} \rightarrow t\bar{t}b\bar{b}$ cross section computed at the next-to-LO (NLO) at the $\sqrt{s} = 13 \text{ TeV}$ LHC Run III, with the couplings $g_{i,j,k}^Q$ and $g_{i,j,k}^q$ chosen so as to maximize it. For comparison, the LO cross section for the process is also shown in the figure.

4 Event Analysis

While limits from the LHC Run 2 analyses have been extracted using the full data sample (140 fb^{-1}), and the Run 3 analyses, which aim to exploit the full luminosity of 300 fb^{-1} , are still ongoing,

	Signal $m_{D,\bar{D}}$				Background		
	500 GeV	600 GeV	700 GeV	800 GeV	$t\bar{t}b\bar{b}$	$t\bar{t}c\bar{c}$	$t\bar{t}jj$
N_{MC}	39200	12600	5040	2100	253400	214200	39480000
N_{PS}	929	324	134	56	2260	484	40199
$N_{M_{WH}}$	663	231	92	36	1635	345	28220
$N_{M_{tH}}$	384	126	47	17	1168	238	19135
$N_{M_{tL}}$	141	44	14	4	580	132	9239
$N_{p_T^b}$	21	11	5	2	10	1	154

Table 3: Cut-flow for the four representative m_D values, corresponding to our standard analysis.

there is a strong expectation that the integrated luminosity of 3000 fb^{-1} at the HL-LHC will greatly extend the scope of the searches for new physics phenomena. In order to estimate the prospects of the (HL-)LHC to observe $D\bar{D}$ pairs in the $t\bar{t}b\bar{b}$ final state, we performed a comprehensive signal-to-background analysis. For maximal reconstruction efficiency of the signal events (S) in our analysis, we assume one of the two W^\pm bosons (e.g., the one from $t \rightarrow Wb$) to decay hadronically, and the other one leptonically. Our final-state is thus comprised of four b -jets, two light jets, a single charged lepton, and missing transverse energy (\cancel{E}_T) from the solitary neutrino. The background events (B) originate from

$$pp \rightarrow t (\rightarrow jjb) \bar{t} (\rightarrow \ell^- \nu \bar{b}) b\bar{b} \text{ and } pp \rightarrow t (\rightarrow jjb) \bar{t} (\rightarrow \ell^- \nu \bar{b}) jj, \quad (15)$$

with the two light jets mis-tagged as b -jets in the latter.

To generate the signal and background events for our MC analysis, we used (as mentioned) `MadGraph5_aMC@NLO` [31] with `NNPDF31_lo_as_0118` parton distribution functions [32], in conjunction with `Pythia-8.2` [41] for parton showering and hadronization, and with `Delphes-3.4.2` [42] for detector emulation. Jet reconstruction was performed using the anti- k_t algorithm [43], while `MadAnalysis5` [44] was used for manipulating the MC data and plotting histograms. For effectively isolating the signal events from the background ones, we implemented the selection criteria detailed below.

4.1 Standard t -quark Reconstruction

We used the ‘standard’ cone size requirement, $R \geq 0.5$, and set the b -tagging efficiency to 85%, c -mistagging rate, $\epsilon_{c \rightarrow b}$, to 25%, and $\epsilon_{u,d,s,g \rightarrow b}$ to 1%, for all the jets (including the b -jets) in the signal as well as the $t\bar{t}jj$ background. We then proceeded as follows.

- PS : Our set of preliminary selections included

$$N(j) \geq 3, N(b) \geq 4, N(\ell) = 1, p_T^j > 20 \text{ GeV}, \text{ and } |\eta^j| < 2.5.$$

Here $N(i)$ is the number of reconstructed objects of the type i , with $i = j, b, \ell$, while p_T and η are the transverse momentum and pseudorapidity, respectively, of a given object.

- M_{WH} : For the hadronic (H) W^\pm decay, from all the possible pairings of the light jets, $j_l j_m$, with $l, m = 1, 2$, the one satisfying $m_{j_l j_m} = m_W \pm 20 \text{ GeV}$ was selected.
- M_{tH} : Out of the four potential jjb_k (for $k = 1, \dots, 4$) combinations of these light-jet pairs with a b -jet, the one with $m_{jjb_k} = m_t \pm 30 \text{ GeV}$ was identified with a t -quark.

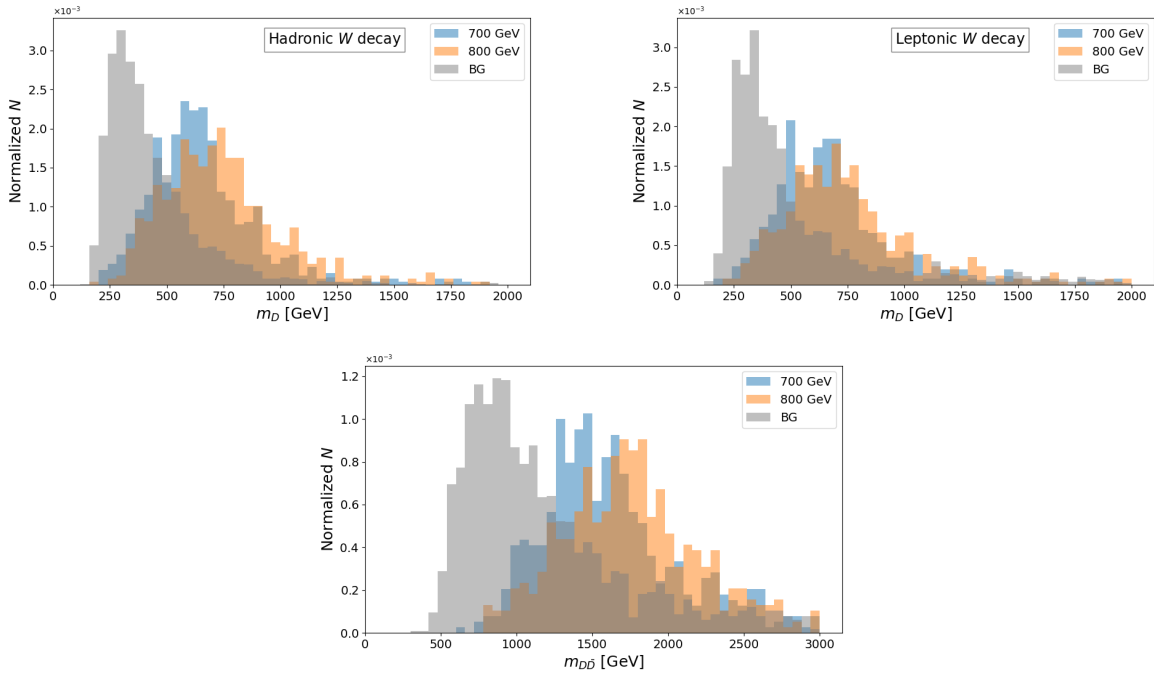


Figure 3: Signal and combined background event distributions for $m_D = 700$ and 800 GeV. Top row corresponds to the D reconstructed from the hadronic (left) and leptonic (right) W^\pm , and bottom row to the $D\bar{D}$ pair.

- $M_t L$: For the leptonic (L) W^\pm , we required $p_T^\ell > 3$ GeV and $|\eta^\ell| < 2.5$, and selected only the events for which $m_{\ell\nu} = m_W \pm 20$ GeV, where m_ν is assumed to be the \cancel{E}_T . The t -quark was then reconstructed as $m_{\ell\nu b_k} = m_t \pm 30$ GeV.
- p_T^b : Finally, we imposed $p_T^{b_{1,2}} > 200$ GeV on the leading and subleading ones among the remaining b -jets. The D and \bar{D} were then selected as those combinations of the two b -jets with the hadronic and leptonic t -quarks that gave $m_{tb} = m_D \pm 50$ GeV and additionally the $|m_D - m_{\bar{D}}|$ closest to zero.

Tab. 3 displays the cut-flow for the signal corresponding to $m_D = \{500, 600, 700, 800\}$ GeV, and for the dominant backgrounds. The distributions of the S and B events for $m_D = 700$ and 800 GeV are shown in Fig. 3, corresponding to the hadronic W^\pm (top left panel) and the leptonic W^\pm (top right panel). The bottom panel similarly illustrates the distributions for the invariant mass of the diquark pair, $m_{D\bar{D}}$.

We further calculated the signal significance, $N_S/\sqrt{N_B}$, where N_S (N_B) is the number of events remaining for the signal ($t\bar{t}b\bar{b}$, $t\bar{t}c\bar{c}$, and $t\bar{t}j\bar{j}$ backgrounds combined) after applying all the selection cuts noted above. These significances, computed using the K -factors for the signal as well as the backgrounds cross sections provided in Refs. [26] and [45], are shown in Tab. 4 assuming integrated luminosities of 140, 300, and 3000 fb^{-1} at the LHC, for $m_D = 500, 600, 700,$ and 800 GeV. We notice a signal significance of $> 5\sigma$ at the HL-LHC for a diquark with up to 600 GeV mass. However, such low masses are already excluded by the ongoing LHC analyses, as noted in the previous section, while our standard event selection criteria fail to yield a statistically substantial isolation of the signal from the background for a higher m_D .

	$m_D = 500 \text{ GeV}$	$m_D = 600 \text{ GeV}$	$m_D = 700 \text{ GeV}$	$m_D = 800 \text{ GeV}$
LHC luminosity	$N_S/\sqrt{N_B} (\sigma)$			
140/fb	2.23	1.20	0.55	0.23
300/fb	3.26	1.75	0.81	0.35
3000/fb	10.33	5.54	2.58	1.11

Table 4: Signal significances obtained with the standard event analysis for the current, design, and high luminosities at the LHC.

	Signal $m_{D,\bar{D}}$				Background	
	700 GeV	800 GeV	900 GeV	1000 GeV	$t\bar{t}b\bar{b}$	$t\bar{t}jj$
N_{MC}	5040	2100	840	420	253400	39480000
N_{PS}	3736	1518	585	282	172373	15462398
N_{M_tH}	117	59	27	16	340	18612
$N_{p_T^b}$	13	11	7	5	5	112

Table 5: Cut-flow for the four representative m_D values, corresponding to our fat-jet analysis.

4.2 Reconstruction of t -quarks from Fat-jets

To potentially obtain a higher signal significance for $m_D > 600 \text{ GeV}$, we adopted an alternative selection strategy incorporating boosted kinematics, wherein the t -quark originating from a relatively heavy D is reconstructed as a single fat-jet, by setting $R \geq 0.8$ in the anti- k_t algorithm. The rest of the analysis commenced as follows.

- PS : The b -tagging and mistagging efficiencies, as well as the p_T^j and η^j requirements remained the same as in the standard analysis above, but the other preliminary selections we imposed now read

$$N(j) \geq 2, N(b) \geq 2, \text{ and } THT > 1400 \text{ GeV},$$

where THT is the hadronic transverse energy.

- M_{tH} : From these events we selected two fat-jets that had invariant masses lying in the $m_t \pm 30 \text{ GeV}$ window as the two t -quark candidates.
- p_T^b : These two fat-jets were then paired with the two leading b -jets, b_1 and b_2 , each required to have $p_T > 150 \text{ GeV}$. The pairing that minimized $|m_{b_i f_j} - m_{b_j f_i}| < 150 \text{ GeV}$ (where the subscript fj implies a fat-jet, and $i, j = 1, 2$) was selected as the $D\bar{D}$ state.

The cut-flow for the events corresponding to $m_D = \{700, 800, 900, 1000\} \text{ GeV}$ in the fat-jet analysis is given in Tab. 5, and the distributions of the $D\bar{D}$ invariant mass for the $m_D = 700$ and 800 GeV signals are shown in Fig. 4.

According to Fig. 5, the signal significances obtained using the fat-jet analysis are considerably enhanced compared to the ones obtained with the standard analysis, for $m_D = 700$ and 800 GeV . Even for $m_D = 900 \text{ GeV}$ this significance is above 3σ , thus implying a fairly strong potential of the HL-LHC to discover a diquark with a sub-TeV mass in the final state considered here.

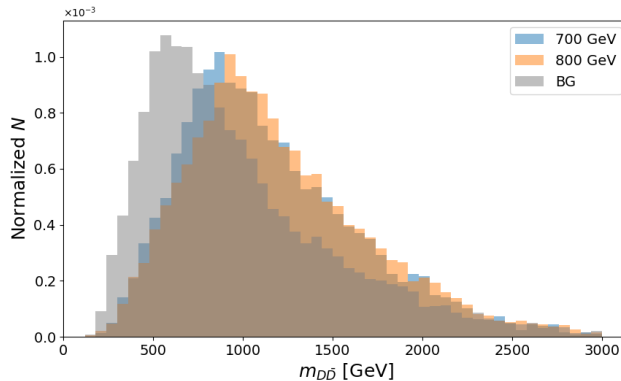


Figure 4: $D\bar{D}$ invariant mass distributions for the $m_D = 700$ and 800 GeV signals and the combined background, using the fat-jet selection criteria.

5 Summary and Conclusions

In this work, we have addressed a significant gap in the literature by performing a detailed phenomenological analysis of the lightest scalar diquark, denoted as D , predicted by the E_6 SSM. Focusing on the $\bar{t}b$ (tb) decay channel of the D (\bar{D}), we established the exclusion limits on its mass based on the most recent LHC data. We then determined the signal significance for the production of pairs of a fairly light (up to 1 TeV) D across various LHC scenarios, including its current and design luminosities, as well as the future HL-LHC with an integrated luminosity of 3000 fb^{-1} .

Our analysis demonstrates that the HL-LHC could achieve a signal significance exceeding 3σ for D masses up to 1 TeV, thus indicating a strong potential for its discovery. Notably, our study goes beyond mere exclusion limits by presenting a robust detector-level analysis, underscoring the feasibility of detecting scalar diquarks of the E_6 SSM framework in realistic experimental conditions.

This study also highlights the importance of diquarks as indicators of beyond the SM physics, and establishes a basis for future research. Its extensions could investigate alternative decay channels, enhanced signal discrimination techniques, and explore wider parameter spaces, thereby advancing our understanding of exotic scalar states, and their relevance to high-energy physics.

Acknowledgments

The work of MA is supported by STEP and OEA from the Abdus Salam ICTP, Trieste, Italy. The work of SK is partially supported by the Science, Technology & Innovation Funding Authority (STDF) under grant number 48173. SM is supported in part through the NExT Institute and the STFC Consolidated Grant No. ST/L000296/1.

References

- [1] J. L. Hewett and T. G. Rizzo, *Low-Energy Phenomenology of Superstring Inspired E(6) Models*, *Phys. Rept.* **183** (1989) 193.
- [2] R. N. Mohapatra, N. Okada and H.-B. Yu, *Diquark Higgs at LHC*, *Phys. Rev. D* **77** (2008) 011701, [0709.1486].

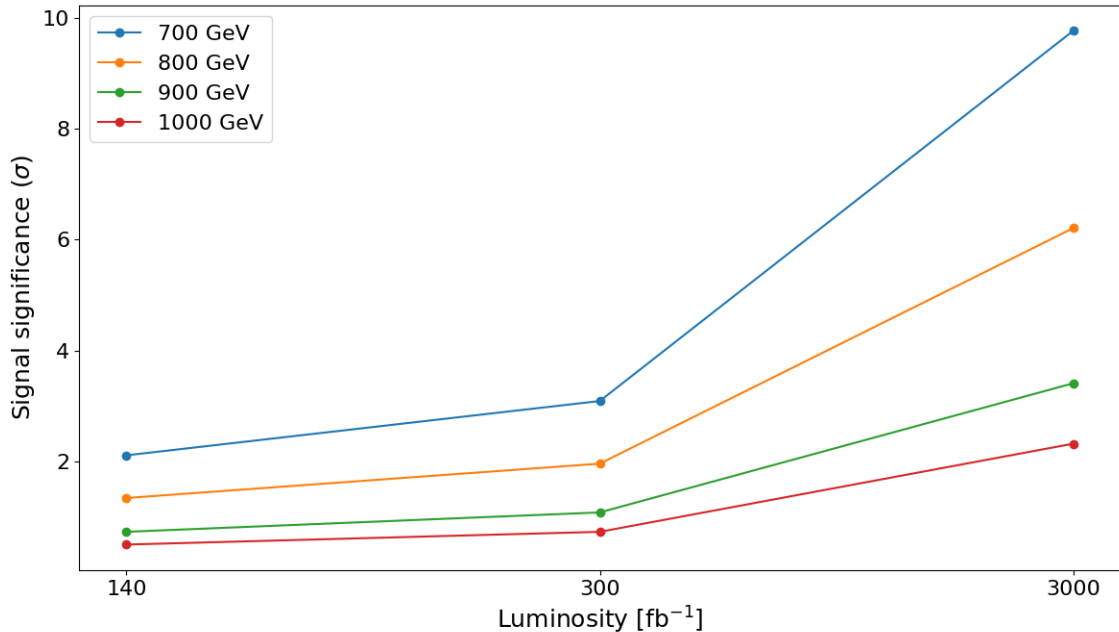


Figure 5: Estimated rise in the signal significances with our fat-jet analysis with increasing luminosity at the LHC, for pair-production of a D with four representative mass values.

- [3] R. Barbier et al., *R-parity violating supersymmetry*, *Phys. Rept.* **420** (2005) 1–202, [hep-ph/0406039].
- [4] I. Baldes, N. F. Bell and R. R. Volkas, *Baryon number violating scalar diquarks at the lhc*, *Phys. Rev. D* **84** (Dec, 2011) 115019.
- [5] R. N. Mohapatra and R. E. Marshak, *Local B-L Symmetry of Electroweak Interactions, Majorana Neutrinos and Neutron Oscillations*, *Phys. Rev. Lett.* **44** (1980) 1316–1319.
- [6] K. S. Babu, P. S. Bhupal Dev and R. N. Mohapatra, *Neutrino mass hierarchy, neutron - anti-neutron oscillation from baryogenesis*, *Phys. Rev. D* **79** (2009) 015017, [0811.3411].
- [7] M. A. Ajaib, I. Gogoladze, Y. Mimura and Q. Shafi, *Observable n - anti-n Oscillations with New Physics at LHC*, *Phys. Rev. D* **80** (2009) 125026, [0910.1877].
- [8] P.-H. Gu and U. Sarkar, *Baryogenesis and neutron-antineutron oscillation at TeV*, *Phys. Lett. B* **705** (2011) 170–173, [1107.0173].
- [9] K. S. Babu and R. N. Mohapatra, *Coupling Unification, GUT-Scale Baryogenesis and Neutron-Antineutron Oscillation in SO(10)*, *Phys. Lett. B* **715** (2012) 328–334, [1206.5701].
- [10] N. B. Beaudry, A. Datta, D. London, A. Rashed and J.-S. Roux, *The $B \rightarrow \pi K$ puzzle revisited*, *JHEP* **01** (2018) 074, [1709.07142].
- [11] C.-H. Chen and T. Nomura, *Left-handed color-sextet diquark in the Kaon system*, *Phys. Rev. D* **99** (2019) 115006, [1811.02315].

- [12] P. S. Bhupal Dev, R. Mohanta, S. Patra and S. Sahoo, *Unified explanation of flavor anomalies, radiative neutrino masses, and ANITA anomalous events in a vector leptoquark model*, *Phys. Rev. D* **102** (2020) 095012, [2004.09464].
- [13] S. M. Barr, *A Survey of a New Class of Models of CP Violation*, *Phys. Rev. D* **34** (1986) 1567.
- [14] S. M. Barr and E. M. Freire, ϵ'/ϵ in *Leptoquark and Diquark Models of CP Violation*, *Phys. Rev. D* **41** (1990) 2129.
- [15] J. Shu, T. M. P. Tait and K. Wang, *Explorations of the Top Quark Forward-Backward Asymmetry at the Tevatron*, *Phys. Rev. D* **81** (2010) 034012, [0911.3237].
- [16] I. Dorsner, S. Fajfer, J. F. Kamenik and N. Kosnik, *Light colored scalars from grand unification and the forward-backward asymmetry in t t -bar production*, *Phys. Rev. D* **81** (2010) 055009, [0912.0972].
- [17] I. Dorsner, S. Fajfer, J. F. Kamenik and N. Kosnik, *Light Colored Scalar as Messenger of Up-Quark Flavor Dynamics in Grand Unified Theories*, *Phys. Rev. D* **82** (2010) 094015, [1007.2604].
- [18] A. Arhrib, R. Benbrik and C.-H. Chen, *Forward-backward asymmetry of top quark in diquark models*, *Phys. Rev. D* **82** (2010) 034034, [0911.4875].
- [19] Z. Ligeti, G. Marques Tavares and M. Schmaltz, *Explaining the t t -bar forward-backward asymmetry without dijet or flavor anomalies*, *JHEP* **06** (2011) 109, [1103.2757].
- [20] K. Hagiwara and J. Nakamura, *Diquark contributions to Top quark charge asymmetry at the Tevatron and LHC*, *JHEP* **02** (2013) 100, [1205.5005].
- [21] G. F. Giudice, B. Gripaios and R. Sundrum, *Flavourful Production at Hadron Colliders*, *JHEP* **08** (2011) 055, [1105.3161].
- [22] H. Tanaka and I. Watanabe, *Color sextet quark productions at hadron colliders*, *Int. J. Mod. Phys. A* **7** (1992) 2679–2694.
- [23] S. Atag, O. Cakir and S. Sultansoy, *Resonance production of diquarks at the CERN LHC*, *Phys. Rev. D* **59** (1999) 015008.
- [24] O. Cakir and M. Sahin, *Resonant production of diquarks at high energy pp , ep and e^+e^- colliders*, *Phys. Rev. D* **72** (2005) 115011, [hep-ph/0508205].
- [25] C.-R. Chen, W. Klemm, V. Rentala and K. Wang, *Color Sextet Scalars at the CERN Large Hadron Collider*, *Phys. Rev. D* **79** (2009) 054002, [0811.2105].
- [26] T. Han, I. Lewis and T. McElmurry, *QCD Corrections to Scalar Diquark Production at Hadron Colliders*, *JHEP* **01** (2010) 123, [0909.2666].
- [27] I. Gogoladze, Y. Mimura, N. Okada and Q. Shafi, *Color Triplet Diquarks at the LHC*, *Phys. Lett. B* **686** (2010) 233–238, [1001.5260].
- [28] S. F. King, S. Moretti and R. Nevzorov, *Theory and phenomenology of an exceptional supersymmetric standard model*, *Phys. Rev. D* **73** (2006) 035009, [hep-ph/0510419].

- [29] S. F. King, S. Moretti and R. Nevzorov, *Exceptional supersymmetric standard model*, *Phys. Lett. B* **634** (2006) 278–284, [[hep-ph/0511256](#)].
- [30] M. Ali, S. Khalil, S. Moretti, S. Munir, R. Nevzorov, A. Nikitenko et al., *TeV-scale leptoquark searches at the LHC and their E_6SSM interpretation*, *JHEP* **03** (2023) 117, [[2302.02071](#)].
- [31] J. Alwall, R. Frederix, S. Frixione, V. Hirschi, F. Maltoni, O. Mattelaer et al., *The automated computation of tree-level and next-to-leading order differential cross sections, and their matching to parton shower simulations*, *JHEP* **07** (2014) 079, [[1405.0301](#)].
- [32] NNPDF collaboration, R. D. Ball et al., *Parton distributions from high-precision collider data*, *Eur. Phys. J. C* **77** (2017) 663, [[1706.00428](#)].
- [33] ATLAS collaboration, G. Aad et al., *Search for charged Higgs bosons decaying into a top quark and a bottom quark at $\sqrt{s} = 13$ TeV with the ATLAS detector*, *JHEP* **06** (2021) 145, [[2102.10076](#)].
- [34] CMS collaboration, A. M. Sirunyan et al., *Search for charged Higgs bosons decaying into a top and a bottom quark in the all-jet final state of pp collisions at $\sqrt{s} = 13$ TeV*, *JHEP* **07** (2020) 126, [[2001.07763](#)].
- [35] W. Porod, *SPheno, a program for calculating supersymmetric spectra, SUSY particle decays and SUSY particle production at e^+e^- colliders*, *Comput. Phys. Commun.* **153** (2003) 275–315, [[hep-ph/0301101](#)].
- [36] W. Porod and F. Staub, *SPheno 3.1: Extensions including flavour, CP-phases and models beyond the MSSM*, *Comput. Phys. Commun.* **183** (2012) 2458–2469, [[1104.1573](#)].
- [37] F. Staub, *SARAH*, [0806.0538](#).
- [38] F. Staub, *SARAH 3.2: Dirac Gauginos, UFO output, and more*, *Comput. Phys. Commun.* **184** (2013) 1792–1809, [[1207.0906](#)].
- [39] F. Staub, *SARAH 4 : A tool for (not only SUSY) model builders*, *Comput. Phys. Commun.* **185** (2014) 1773–1790, [[1309.7223](#)].
- [40] F. Staub, *Exploring new models in all detail with SARAH*, *Adv. High Energy Phys.* **2015** (2015) 840780, [[1503.04200](#)].
- [41] T. Sjostrand, S. Mrenna and P. Z. Skands, *PYTHIA 6.4 Physics and Manual*, *JHEP* **05** (2006) 026, [[hep-ph/0603175](#)].
- [42] DELPHES 3 collaboration, J. de Favereau, C. Delaere, P. Demin, A. Giammanco, V. Lemaitre, A. Mertens et al., *DELPHES 3, A modular framework for fast simulation of a generic collider experiment*, *JHEP* **02** (2014) 057, [[1307.6346](#)].
- [43] M. Cacciari, G. P. Salam and G. Soyez, *The anti- k_t jet clustering algorithm*, *JHEP* **04** (2008) 063, [[0802.1189](#)].
- [44] E. Conte, B. Fuks and G. Serret, *MadAnalysis 5, A User-Friendly Framework for Collider Phenomenology*, *Comput. Phys. Commun.* **184** (2013) 222–256, [[1206.1599](#)].
- [45] D. Choudhury, K. Deka and L. K. Saini, *Boosted four-top production at the LHC: A window to Randall-Sundrum or extended color symmetry*, *Phys. Rev. D* **110** (2024) 075020, [[2404.04409](#)].